Extended Abstracts of the 2015 International Conference on Solid State Devices and Materials, Sapporo, 2015, pp646-647

Band-to-Band Graphene Resonant Tunneling Field Effect Transistor

Shunei Suzuki,[1] Manoharan Muruganathan,[1] Shunri Oda[2] and Hiroshi Mizuta [1,3]

[1] Japan Advanced Institute of Science and Technology, Nomi Asahidai 1-1, Ishikawa, Japan
[2]Quantum Nanoelectronics Research Center, Tokyo Institute of Technology, Ookayama, Meguro-ku, Tokyo, Japan
[3]Nanoelectronics and Nanotechnologies Research Group, Faculty of Physical Sciences and Engineering, University of Southampton, Highfield, Southampton, UK
E-mail: shun-suzuki@jaist.ac.jp

Abstract

Band-to-band graphene resonant tunneling field effect transistor (GRTFET) is proposed and its tunneling mechanism is studied based on Extended Hückel tight-binding model. Electrostatic difference potential analysis showed the modulation of the potential barriers for the onset of the carrier tunneling. Resonant tunneling states are formed by channel intrinsic region 2*p* orbitals in the GRTFET operation regime, which lead to carrier transmission across the channel. This is confirmed by molecular projected self-consistent Hamiltonian states. Furthermore, we obtained subthreshold slope (SS) of 43.7 mV/dec, OFF current 8 pA/µm, ON current 11.6 mA/µm, ON/OFF ratio 1.4×10^{9}.

1. Introduction

As CMOS is downscaled below 50 nm, its stand-by OFF state power is catching up to ON state dynamic operation power [1]. In order to overcome this issue, we have to realize low OFF state current device with small subthreshold value. In this direction, tunnel field effect transistor (TFET) is an important candidate. In TFET, carrier tunneling set the device on-state condition, which is controlled by the gate voltage (Fig.1). As SS of TFET is decided by the modulation efficiency of the Band-to-Band tunneling currents, realizing SS < 60 mV/dec is theoretically possible and off-state leak current is exponentially reduced depending on the bandgap of the intrinsic channel.

Si-based TFET has been studied [2], however it suffers from low on-state current due to the large band gap of Si. In contrast, graphene-based TFET is expected to realize a high tunneling current in an on-state due to the small band gap in the graphene nanoribbon (GNR). Our proposed band-to-band tunneling GRTFET is shown in Fig. 2. Gates 1 and 3 will be used to realize p and n regions in the zigzag GNR (ZGNR) regions. Carrier tunneling will be controlled by Gate 2 in the armchair GNR (AGNR) region.

2. Computational method

In this study, we used self-consistent Extended Hückel tight-binding model implemented in Atomistix ToolKit (ATK) 14.1 to analyze the tunneling mechanism of GRTFET [3]. Non-equilibrium Green's function formalism is used to calculate the device transport characteristics. Source and drain bias voltages, V_{G1} and V_{G2} values shown in Fig. 2 are used for the all other simulations at 300 K. 3-ZGNRs are used to realize p and n type doped regions and 4-AGNR is employed for the intrinsic channel region. Electrodes are constructed using ZGNRs.

3. Results and discussion

At first, modulation of the channel potential individually by three gates is confirmed by analyzing the electrostatic difference potentials (Fig. 3). By applying -1.0 V and 1.0 V to Gates 1 and 3, p and n doped regions are achieved, respectively. By controlling the Gate2, potential barrier is overcome for the carrier tunneling between source and drain (Figs. 3b & c). In order to understand the carrier transmission across the intrinsic channel, device density of states (DOS) is calculated (Fig. 4). The major contribution comes from 2*p* orbitals of the channel. As the control gate voltage is increased then the emergence of the new peaks can be noticed, which are marked by arrow A. The origin of these peaks is studied using projected DOS analysis. 2*p* orbitals of the intrinsic channel leads to these resonant peaks (Fig. 5).

To further understand the energy levels in the channel with the applied gate voltages, molecular projected self-consistent Hamiltonian states are calculated (Fig. 6). At the resonant peak energy, the presence of the energy states across the entire channel can be clearly noticed in Fig. 6(b). This is important for the carrier transmission across the source and the drain. Transmission spectra for various Gate 2 voltages are shown in Fig. 7. Emergence of the resonant states and its role to the increase the transmission value in the tunnel region can be noticed. The gate characteristic of GRTFET is shown in Fig. 8 along with transconductance. From this characteristics, steep switching properties with SS = 43.7 mV/dec is obtained. The SS for our GRTFETs is governed by the width and peak transmission value of the 1st resonant tunneling state and its energy modulation efficiency via Gate 2. Moreover, we obtained low OFF current (V_{G2}=0V, I_{OFF} = 8.2 pA/µm) and high ON current (V_{G2}=5.0V, I_{ON} =11.6 mA/µm).

In conclusion, band-to-band graphene resonant tunneling FET operation was proposed and studied using the tight-binding model. Resonant tunneling states originated from the channel intrinsic region 2*p* orbitals plays the important role for the high-performance GRTFET operation.

Acknowledgements
This work is supported by the Center of Innovation Program (COI) of the Japan Science and Technology Agency.

References

[1] Ruchir Puri, *et al.*, *Design Automation Conference*, pp. 285-288, 2005.
[2] Yukinori Morita, *et al*, *IEEE Electron Device Letters*, **35,** 7**,** 2014.
[3] K. Stokbro, D.E. Petersen, S. Smidstrup, A. Blom, M. Ipsen, and K. Kaasbjerg, *Phys. Rev.* B, 82, 075420, 2010.

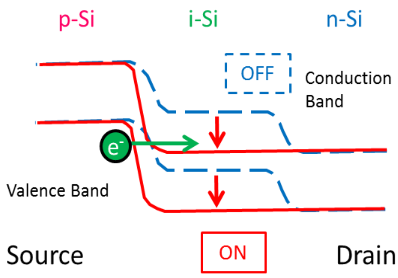

Fig. 1 Electron tunneling in TFET

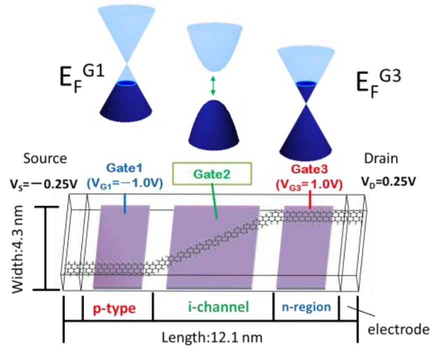

Fig. 2 Simulated GRTFET atomistic structure

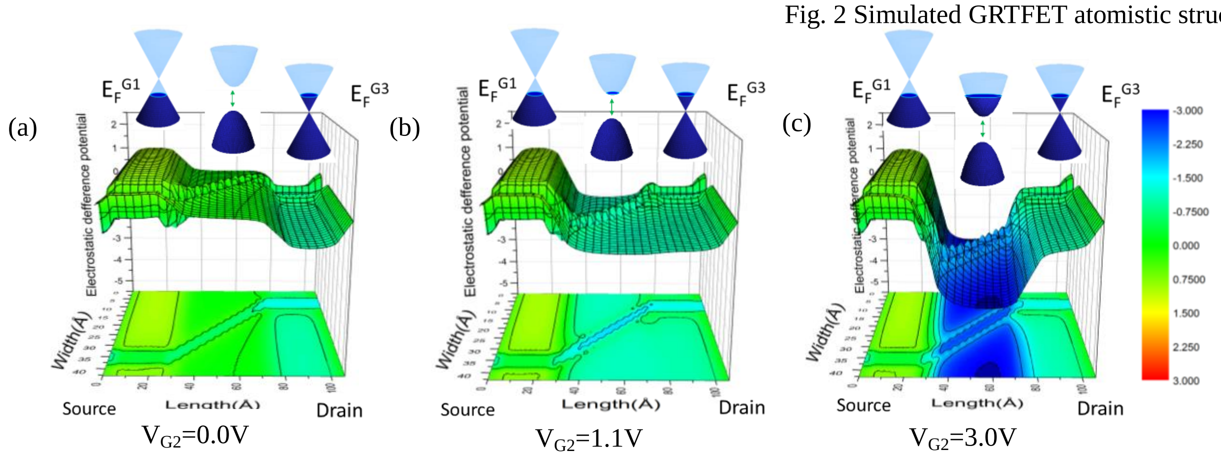

Fig. 3 Electrostatic Difference Potential across the GRTFET channel for V_{G1}=－1.0V and V_{G3}=1.0V

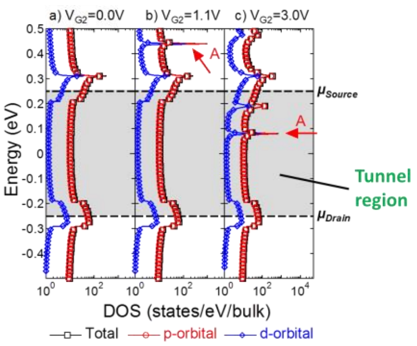

Fig. 4 Device density of states (DOS)

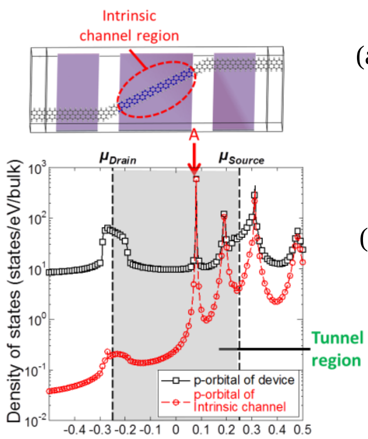

Fig. 5 DOS of intrinsic channel (V_{G2}=3.0V)

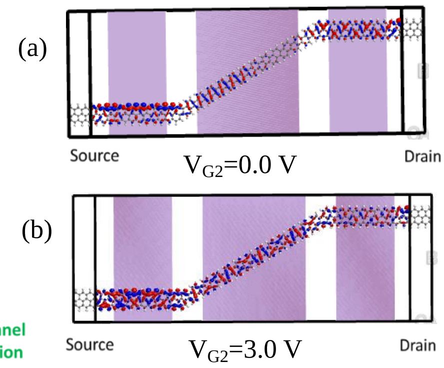

Fig. 6 Molecular projected self-consistent Hamiltonian states (Isovalue=0.02)

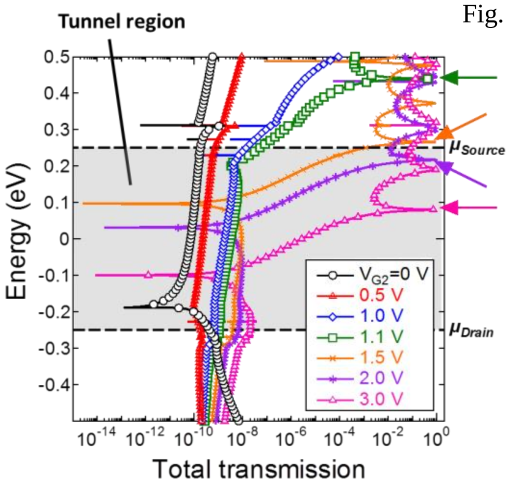

Fig. 7 Transmission spectra for different V_{G2}

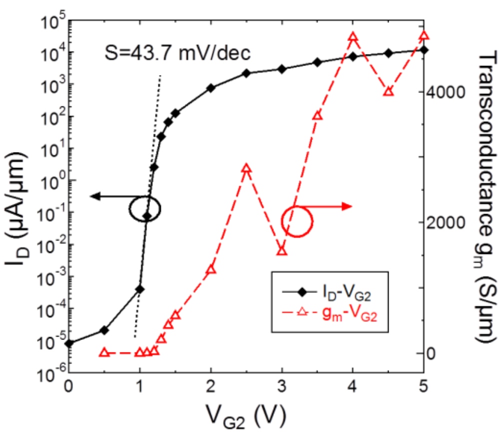

Fig. 8 I_D-V_{G2} and g_m-V_{G2} characteristics